Original Article

Access this article online
Quick Response Code:

Website:
https://eurasianjpulmonol.org
DOI:
10.14744/ejp.2024.30589

Strain elastography in detecting the nature of peripheral lung lesions: Unveiling the potential of innovative diagnosis

Mona Saeed El Hoshy[1], Essam Gouda Hassanein[1], Ayman Ibrahim Baess[1], Doaa M. Emara[2], Ahmed Farag Abouelnour[1]

ORCID:
Mona Saeed El Hoshy: 0009-0005-2787-5207
Essam Gouda Hassanein: 0009-0006-7088-8473
Ayman Ibrahim Baess: 0000-0002-4297-8061
Doaa M. Emara: 0000-0002-0012-6995
Ahmed Farag Abouelnour: 0009-0002-7097-4460

Abstract:

BACKGROUND AND AIM: Imaging techniques play a crucial role in assessing lung structure and function, particularly in diagnosing respiratory diseases. Among these, ultrasound strain elastography (SE) presents a promising method for evaluating peripherally located lung parenchymal lesions and distinguishing between benign and malignant pathologies. This study aims to explore the applicability and reliability of ultrasound elastography (USE) in tissue differentiation and to establish a strain ratio (SR) cutoff value for accurate classification.

METHODS: A diagnostic accuracy study was conducted on a cohort of 138 patients aged 18 years and older to assess the efficacy of SR analysis in determining optimal cutoff points for differentiating between benign and malignant lesions. Sensitivity, specificity, negative predictive value (NPV), positive predictive value (PPV), area under the curve (AUC), and accuracy were determined using receiver operating characteristic (ROC) analysis.

RESULTS: Tissue stiffness was assessed using SE, revealing that malignant lesions exhibited a stiffer pattern compared to benign ones. An SR cutoff value of ≥1.75 was determined for diagnosing malignant peripheral lesions. The sensitivity, specificity, PPV, and NPV were 98.67%, 82.54%, 87.1%, and 98.1%, respectively.

CONCLUSIONS: The use of SE can assist in classifying a peripheral parenchymal lung lesion as benign or malignant based on the SR.

Keywords:

Elastography, lung ultrasonography, peripheral lung lesions, strain ratio

[1]Department of Chest Diseases, Alexandria University Faculty of Medicine, Alexandria, Egypt, [2]Department of Radiodiagnosis and Intervention, Alexandria University, Alexandria, Egypt

Address for correspondence:
Dr. Ahmed Farag Abouelnour, Department of Chest Diseases, Alexandria University Faculty of Medicine, Alexandria, Egypt.
E-mail: abouelnourahmed@gmail.com

Received: 30-10-2024
Revised: 18-12-2024
Accepted: 21-12-2024
Published: 04-08-2025

How to cite this article: El Hoshy MS, Hassanein EG, Baess AI, Emara DM, Abouelnour AF. Strain elastography in detecting the nature of peripheral lung lesions: Unveiling the potential of innovative diagnosis. Eurasian J Pulmonol 2025;27:77-87.

Introduction

Lung ultrasonography (LUS) has gained prominence in emergency rooms and critical care units, overcoming traditional limitations posed by air-filled lung tissue. Recent advancements, such as high-frequency transducers and sophisticated image processing, have revolutionized lung examination, enabling a detailed assessment of the pleural line and pleural space. The development of ultrasound elastography (USE) in the 1990s has further enhanced diagnostic capabilities by providing precise measurements of tissue stiffness, aiding in the differentiation between soft and hard lesions.[1–3]

Conventional LUS is highly sensitive for detecting tumors; however, it does not provide reliable information about tissue firmness. USE, on the other hand, is an ultrasound-based technique designed to visualize the elasticity characteristics of different tissue types. It was developed as a non-invasive method to assess tissue stiffness.[4–6]

Tissue stiffness is typically represented as tissue strain, which can be a subjective measurement due to variations in the compression applied by the ultrasound probe. The SR, however, provides an objective semi-quantitative measurement, reflecting the difference in tissue strain compared to the surrounding tissue on USE images.[2,4]

The SR is calculated as the relative difference in strain between a lesion and reference normal tissue at the same depth, under the same stress applied by compression. Elastography and the SR have been extensively used in imaging the breast, liver, and thyroid gland, primarily for diagnosing malignancies. However, only a few studies have explored the use of elastography and the SR for diagnosing peripheral lung lesions.[2,7,8]

Study Objective

This research aims to assess the efficacy and reliability of non-invasive USE in distinguishing between different tissue types by analyzing the varying strain patterns of soft and hard lesions. The study focuses on determining an optimal cutoff value for the strain ratio (SR) to achieve accurate classification using USE.

Materials and Methods

This is a prospective diagnostic accuracy study with comparisons to gold standard tests. All patients, selected through cross-sectional sampling, provided informed consent before participation, and the study protocol was approved by the Ethics Committee of Alexandria University (Approval Number: 0201692, Date: 16.06.2022). The sample size was calculated by the Medical Research Institute and the Biomedical Informatics and Medical Statistics Department. This study was conducted in accordance with the Declaration of Helsinki. This work was produced without the assistance of artificial intelligence (AI)-assisted technologies, including large language models (LLMs), chatbots, or AI-based image creators.

The study included 138 cases with peripheral subpleural lesions. A thorough history was obtained from the participants, including personal data, symptoms relevant to underlying respiratory disorders, and a history of previous malignancy. A complete physical examination, routine laboratory tests, and imaging modalities, including chest X-ray and computed tomography (CT) chest scan, were conducted.

Histopathological biopsies were obtained through flexible bronchoscopy, and when indicated, image-guided biopsies were performed trans-thoracically using a semi-automatic needle biopsy. Benign lesions, such as consolidation, bronchiectasis, and distal atelectasis, were documented and monitored until clinical resolution and/or radiological improvement (Table 1).[9]

Ultrasound imaging was performed before biopsy, and all examinations were conducted by the same examiner using a SonoScape machine (M22EXP, China) equipped with a curvilinear probe operating within a frequency range of 2–5 MHz.

After applying ultrasound gel to ensure optimal contact between the transducer and the skin, B-mode sonography was initially performed to locate the tumor. For cases confirmed by biopsy, this also facilitated the identification of the needle entry point and insertion path. Elastography was then conducted using freehand manual compression, with the radiologist applying light vertical pressure to the mass using the transducer. During imaging, the strain indicator on the screen was monitored. The images were displayed in dual mode, showing both the B-mode sonogram and the elastography image, with elasticity represented on a color scale from red (softest) to blue (hardest). Patient movement was minimized during the procedure [Fig. 1].[2,10]

Table 1: Distribution of malignant tissue types and computed tomography (CT) findings of pulmonary lesions

Lesion classification	n	%
	n=75	
A) Types of malignant tissues		
Adenocarcinoma	23	30.6
Metastatic lesions	15	20.0
Small cell lung carcinoma (SCLC)	12	16.0
Squamous cell carcinoma (SCC)	10	13.3
Non-small cell lung carcinoma (NSCLC)	9	12.0
Undifferentiated carcinoma (UC)	5	6.7
Lymphoma	1	1.3
	n=63	
A) CT features of benign lesions		
Consolidation	34	54.0
Cavitary lesions	11	17.5
Distal atelectasis	9	14.3
Bronchiectasis	7	11.1
Progressive massive fibrosis	1	1.6
Thymoma	1	1.6

Distribution of lesions based on types of malignant lesions and computed tomography (CT) features of benign lesions. n: Number

Using the strain elastography (SE) approach, a region of interest (ROI) was selected and compared to a manually selected surrounding reference tissue, denoted as the reference (Ref) tissue.

The SE characteristics were classified into three types based on elasticity and the proportion of the blue component:

- Type I: Indicates very soft tissue with high elasticity, characterized by a predominantly red color, with the blue component covering less than 25% of the lesion area.
- Type II: Represents moderately soft tissue with moderately high elasticity, showing an increasing blue content within the lesion.
- Type III: Describes very hard tissue with low elasticity, predominantly blue (>75% of the total ROI area), with only a few small red regions.[5,11]

The SR value was calculated and correlated with the final diagnosis. Sensitivity, specificity, negative predictive value (NPV), positive predictive value (PPV), area under the curve (AUC), and accuracy were determined using receiver operating characteristic (ROC) analysis for all lesions.

The performance of the SR cutoff value was assessed by splitting the final dataset into two equal halves: one half for determining the SR cutoff values and the other half for validating the SR. The performance of the SR was evaluated based on sensitivity, specificity, NPV, PPV, and accuracy, with their respective 95% confidence intervals (CIs). The AUC was also computed for continuous variables.[12]

Statistical analysis

Data were entered into a computer and analyzed using IBM SPSS software version 20.0 (Armonk, NY: IBM Corp). Qualitative data were described using numbers and percentages. The Kolmogorov-Smirnov test was applied to verify the normality of distribution. Quantitative data were presented using the range (minimum and maximum), mean, standard deviation, median, and interquartile range (IQR). The significance of the obtained results was determined at the 5% level.

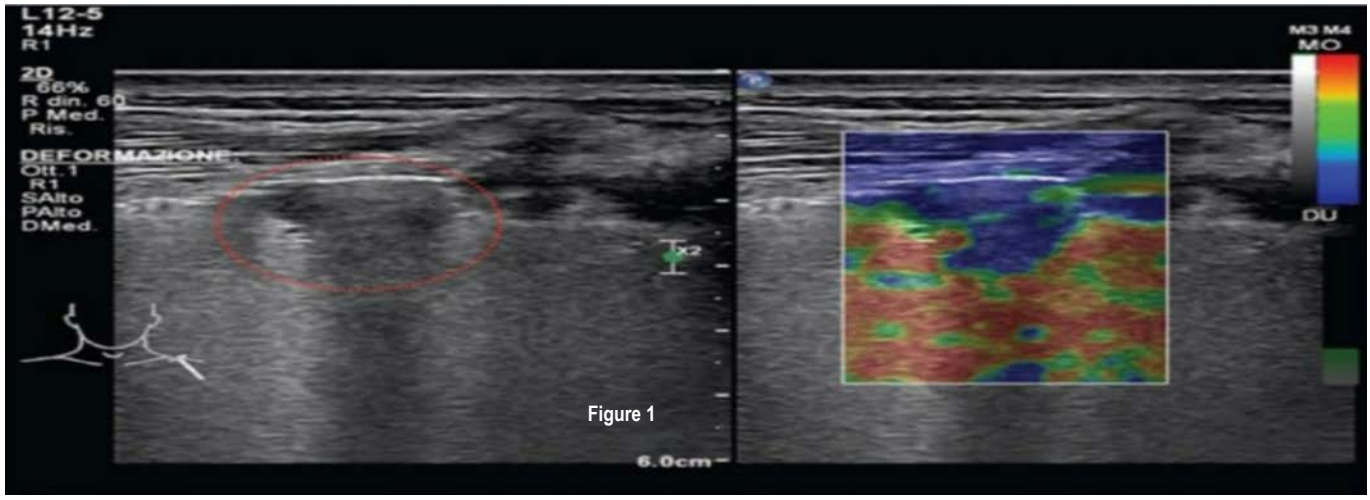

Figure 1

Figure 1: Dual-mode ultrasonography of a soft tissue lesion – B-mode imaging and corresponding strain elastography. Figure 1 illustrates the visualization of a soft tissue lesion using dual-mode ultrasonography with B-mode imaging alongside the corresponding SE image

SE: Strain elastography

Table 2: Baseline characteristics of the study population

Patient characteristics	n	%
	n=138	
Gender*		
Male	102	73.9
Female	36	26.1
Age (mean)*	55.1 years	
Smoking status*		
Smokers	91	65.9
Non-smokers	47	34.1
	n=66	
Comorbidities*		
Hypertension	36	26.1
Diabetes mellitus	28	20.3
CKD	1	0.7
Liver cirrhosis	8	5.8
Lymphoma	2	1.5
Leukemia	3	2.2
Ischemic heart disease	11	8.0
Systemic lupus	1	0.7
Deep vein thrombosis	3	1.5

Age is presented as the mean value. Comorbidity data reflect the total number of patients with each condition, with some patients having multiple comorbidities. CKD: Chronic kidney disease

Several statistical tests were applied based on the nature of the data. The Chi-square test was used to compare categorical variables across different groups. When more than 20% of the cells had expected counts below 5, Fisher's Exact correction was applied to refine the Chi-square results.

For comparing non-normally distributed quantitative variables between the two study groups, the Mann-Whitney test was used.

To investigate the SR cutoff value, a ROC curve was generated to illustrate the performance of the SR in diagnosing malignant peripheral lung lesions based on its sensitivity and specificity.

Results

A total of 138 patients (102 males and 36 females) were included in the study, conducted between November 2022 and September 2023. The patients' ages ranged from 18 to 95 years, with a mean age of 55.07±15.85 years. The baseline characteristics of the patients are listed in Table 2.

The types of malignant tissues and the corresponding CT findings of benign pulmonary lesions are illustrated in Table 1, detailing the distribution of malignant and benign lesions along with their characteristic features.

Table 3: Classification of lesions by transthoracic elastography based on tissue stiffness

Lesion type (by elastography)	n	p	%
Type I (soft lesion)	51	<0.001*	37.0
Malignant	0		
Benign	51		
Type II (intermediate lesion)	56		40.6
Malignant	46		
Benign	10		
Type III (hard lesion)	31		22.5
Malignant	29		
Benign	2		

P value calculated using the chi-square test. A p value <0.001 indicates a statistically significant difference in the distribution of lesion types between malignant and benign cases.

All lesions identified through radiological examinations, including X-ray, CT chest scans, and positron emission tomography-computed tomography (PET-CT) scans, were detected using elastography in the examined cases. Tissue stiffness was assessed using SE, with the following findings: 31 lesions exhibited a hard pattern (Type III), 56 lesions showed an intermediate pattern (Type II), and 51 lesions displayed a soft pattern (Type I).

Lesions classified as Type I (soft pattern on SE) were diagnosed as benign (n=51) based on histopathological diagnosis or clinical follow-up. Type II lesions (intermediate pattern on SE, n=56) were diagnosed as malignant in 46 cases and benign in 10 cases. Type III lesions (hard patterns on SE, n=31) were diagnosed as malignant in 29 cases and benign in two cases. SE values were significantly higher in malignant lesions compared to benign lesions, with a statistically significant difference ($p<0.001$) (Table 3).

The optimal performance of the SR for diagnosing malignant peripheral lesions was observed with a value set at ≥2.2±0.45. However, an SR cutoff value of ≥1.75 achieved the highest sensitivity (Table 4).

The following ROC curve illustrates the performance of SR elastography based on sensitivity and specificity in diagnosing malignant peripheral lung lesions [Fig. 2].

The range and median SR values for each lesion type indicate distinct differences between benign and malignant lesions. Benign lesions exhibited a lower strain ratio, whereas malignant lesions had a higher strain ratio.

Table 4: Prognostic performance of strain ratio for differentiating malignant (n=75) and benign (n=63) lesions

Strain ratio	AUC	p	95% CI	Cut-off	Sensitivity	Specificity	PPV	NPV	Accuracy
Strain ratio (>2.65)	0.912	<0.001*	0.854–0.970	>2.65	38.67	93.65	87.9	56.19	63.8%
Strain ratio (>2.5)	0.912	<0.001*	0.854–0.970	>2.5	60.0	90.48	88.2	65.5	74.0%
Strain ratio (>1.75)	0.912	<0.001*	0.854–0.970	>1.75	98.67	82.54	87.1	98.1	91.3%

This table presents diagnostic performance metrics for different strain ratio cutoff values in detecting malignant lesions. Area under the curve (AUC) indicates the accuracy of the test and p<0.001 confirms the statistical significance of the findings. Sensitivity, specificity, positive predictive value (PPV), and negative predictive value (NPV) are calculated based on the specified cutoff points for the strain ratio. CI: Confidence interval

This contrast was statistically significant, suggesting that strain ratio could serve as a useful parameter for differentiating between benign and malignant lesions [Fig. 3].

To validate the adoption of a SR of ≥1.75 as the optimal cutoff value for sensitivity, the total of 138 patients was divided into two equal groups to assess the accuracy, sensitivity, and specificity of the selected cutoff value.

For the initial 69 lesions (Malignant:Benign = 40:29), the optimal SR threshold for diagnosing malignant peripheral lesions was ≥1.75 (Table 5) [Fig. 4].

Using an SR cutoff value of ≥1.75 to predict malignant lesions, the remaining 69 lesions demonstrated comparable accuracy to the initial group, with an overall accuracy of 85.5% (Table 6, Figs. 5-7).

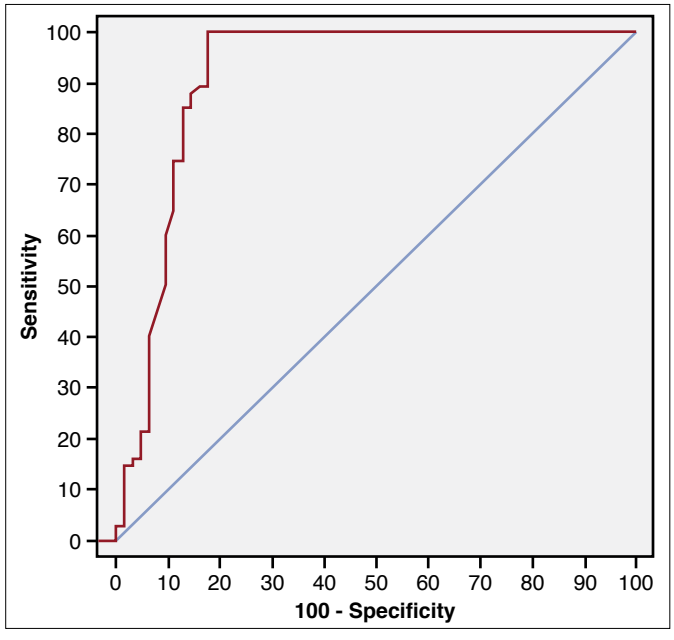

Figure 2: Receiver operating characteristic (ROC) curve for the strain ratio in diagnosing malignant (n=75) and benign (n=63) lesions. Figure 2 presents the ROC curve for the strain ratio in diagnosing malignant (n=75) and benign (n=63) lesions. The ROC curve demonstrates the test's diagnostic performance, with the AUC indicating the accuracy of the strain ratio in distinguishing between malignant and benign cases
AUC: Area under the curve

Discussion

Real-time tissue elastography is an innovative technique that converts echo signals into dynamic color images, where the color spectrum shifts from red to blue, indicating varying tissue softness and hardness. Malignant tumors often exhibit increased firmness, a characteristic that enables elastosonography to efficiently identify these lesions.[13–15]

Among the patients enrolled in this study, 75 had malignant peripheral lesions (54.3%), while 63 had benign lesions (45.6%). This finding is consistent with the study by Lim et al.,[16] where 38 out of 70 patients were diagnosed with malignant peripheral lesions, accounting for 54% of the total cohort.

In this study, consolidation was the most commonly observed benign lesion, while adenocarcinoma was the most frequently diagnosed malignant lesion. These

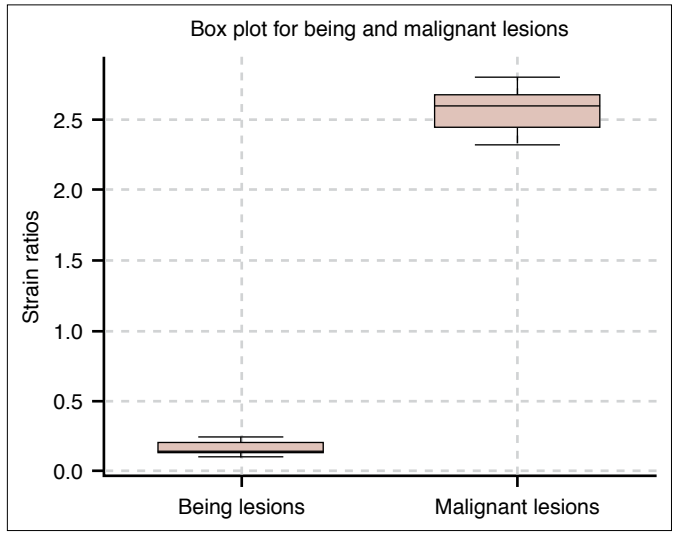

Figure 3: Median and range of strain ratio (SR) for benign and malignant lesions. Figure 3 presents a box plot for benign and malignant lesions. It illustrates the range and median strain ratio for each lesion type. The SR for benign lesions ranges from 0.1 to 0.24, with a median of 0.15, while for malignant lesions, it ranges from 2.33 to 2.80, with a median of 2.60 (p<0.001)

Table 5: Prognostic performance of strain ratio (SR) in predicting malignant versus benign lesions (40 malignant, 29 benign) among the initial 69 cases

Results	AUC	p	95% CI	Cutoff value	Sensitivity	Specificity	PPV	NPV	Accuracy
Value	0.995	<0.001*	0.984–1	≥1.75	97.50%	96.55%	97.50%	96.6%	97%

This table presents the prognostic performance of the strain ratio in predicting malignant and benign lesions among the initial 69 cases. Area under the curve (AUC) represents the diagnostic accuracy of the test. Sensitivity, specificity, positive predictive value (PPV), and negative predictive value (NPV) are reported for a strain ratio (SR) cutoff value of ≥1.75. CI: Confidence interval

Table 6: Agreement (sensitivity, specificity, and accuracy) for strain ratio validation in the remaining malignant (n=35) and benign (n=34) cases

	Diagnosis				Sensitivity	Specificity	PPV	NPV	Accuracy
	Benign (n=34)		Malignant (n=35)						
	No	%	No	%					
Strain ratio									
≤1.75	24	70.6	0	0.0	100.0	70.6	77.8	100.0	85.5
>1.75	10	29.4	35	100.0					

This table presents the diagnostic performance of the strain ratio (SR) in predicting benign and malignant lesions for the remaining cases (n=69). Sensitivity, specificity, positive predictive value (PPV), negative predictive value (NPV), and accuracy are calculated based on a strain ratio cutoff value of <1.75 and ≥1.75. These values represent the percentage of correctly diagnosed cases within each category

findings contrast with the study by Sperandeo et al.,[17] in which adenocarcinoma was most prevalent, followed by squamous cell carcinoma and large cell carcinoma, with small cell carcinoma exhibiting a higher prevalence among all malignant peripheral lesions.

In line with our study, He et al.[9] examined central lesions using endoscopic ultrasound (EBUS) elastography in 57 patients. Among them, 36 were diagnosed with malignancies (63%), with small cell carcinoma being more prevalent than squamous cell carcinoma. Similarly, consolidation was the most common benign lesion, followed by cavitary lesions, findings that are consistent with our study.

Tissue stiffness was assessed using SE. Parenchymal lesions were classified into Type I, II, and III based on the proportion of the blue component observed in the SE color-coding system. The correlation between color coding and final lesion diagnosis was statistically significant ($p<0.001$).[11]

Similarly, Boccatonda et al.[11] conducted a study involving 14 patients, where nine had Type III (hard) lesions, three had Type II lesions, and two had Type I (soft) lesions. The diagnostic performance of SE for identifying malignant lesions demonstrated an area under the ROC curve of 0.7. Furthermore, Park et al.[5] showed that SE is an effective technique for assessing superficial soft tissue lesions, emphasizing that malignant lesions tend to be stiffer on SE.

In an alternative retrospective study conducted by Wei et al.,[18] the diagnostic efficacy of SE was evaluated in 91 peripheral lung lesions identified via CT chest scan or chest X-ray. Among these, 36 were diagnosed as benign lesions,

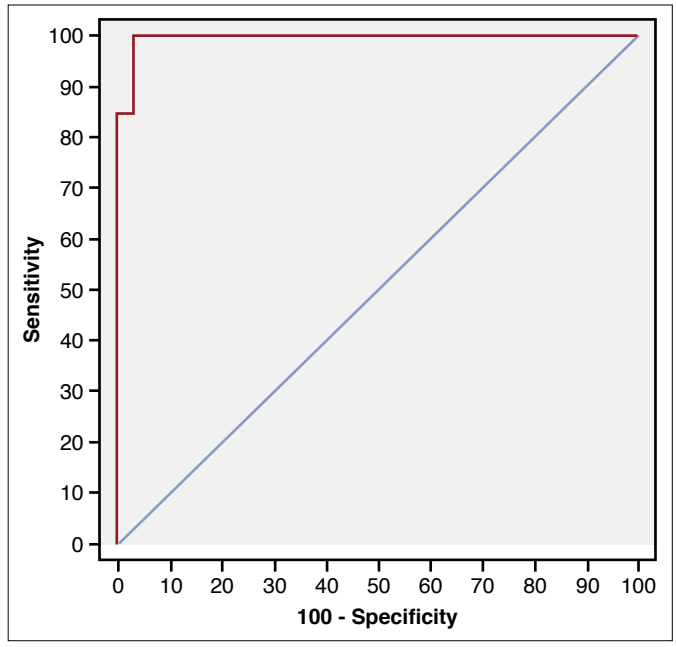

Figure 4: Receiver operating characteristic (ROC) curve for strain ratio in predicting malignant and benign lesions among the initial 69 cases (40 malignant, 29 benign). Figure 4 displays the ROC curve for the strain ratio in differentiating malignant and benign lesions among the initial 69 cases (40 malignant, 29 benign). The curve illustrates the diagnostic ability of the strain ratio, with the area under the curve (AUC) reflecting the test's accuracy

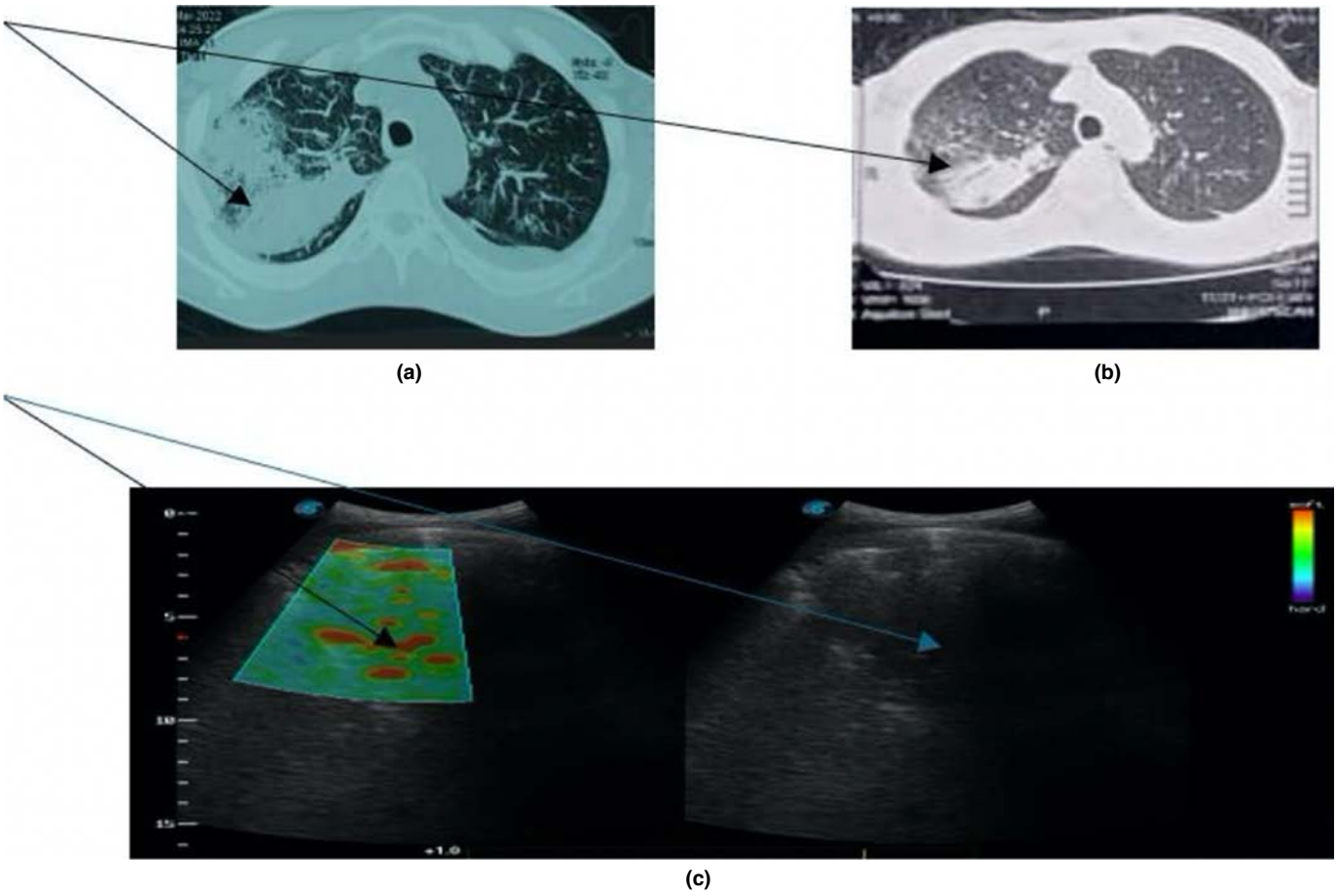

Figure 5: Computed tomography (CT) chest of a consolidation pre- and post-antimicrobial therapy with ultrasound elastography examination of the same lesion. Figure 5 describes a patient presenting with high-grade fever, productive cough with hemoptysis, and right-sided chest pain. (a) Initial chest CT scan (lung window) upon admission showed extensive right upper consolidation with air bronchogram. (b) A follow-up CT scan after antimicrobial therapy demonstrated significant regression of the consolidation, aligning with clinical improvement and a marked decrease in C-reactive protein (CRP) levels. (c) Ultrasound elastography (USE) with a strain ratio (SR) of 0.12 and B-mode ultrasound imaging revealed an echogenic air bronchogram, while the corresponding elastography image displayed no blue component, indicating that the lesion was relatively soft, represented in red

while 55 were malignant, confirmed through histopathological validation. The study concluded that relying solely on color coding in SE was insufficient for differentiating between malignant and benign peripheral lung lesions.

Within the scope of our study, histopathological biopsy served as the gold standard for patient diagnosis. However, 15 patients were found to have metastatic lesions that did not require biopsy confirmation. These lesions exhibited increasing size during follow-up, with diagnoses corroborated by both oncologists and radiologists. Additionally, one patient was diagnosed with lymphoma, which showed a regressive course following chemotherapy.

Similarly, Lim et al.[16] aimed to evaluate the SR in relation to different pulmonary morphologies, relying on both radiological evidence and histopathological diagnosis. For patients ultimately diagnosed with benign peripheral lesions without histopathological analysis, rigorous clinical and radiological follow-up was conducted until complete resolution.[9,16]

Zhou et al.[19] used histopathological final diagnosis as the gold standard for evaluating EBUS elastography in all examined subjects. Additionally, Sperandeo et al.[20] and Wei et al.[18] relied on transthoracic tissue biopsy as the gold standard to assess the efficacy of ultrasound elastography. Similarly, Sperandeo et al.,[17] Boccatonda et al.,[11] and Wei et al.[18] all utilized a transthoracic guided biopsy approach as the gold standard for thoracic ultrasound SE examination.[17]

We aimed to establish SR cutoff values by comparing various lesions identified as the ROI with normal healthy surrounding tissue, denoted as the Ref region. Initially, a median cutoff value was determined from a cohort of 138

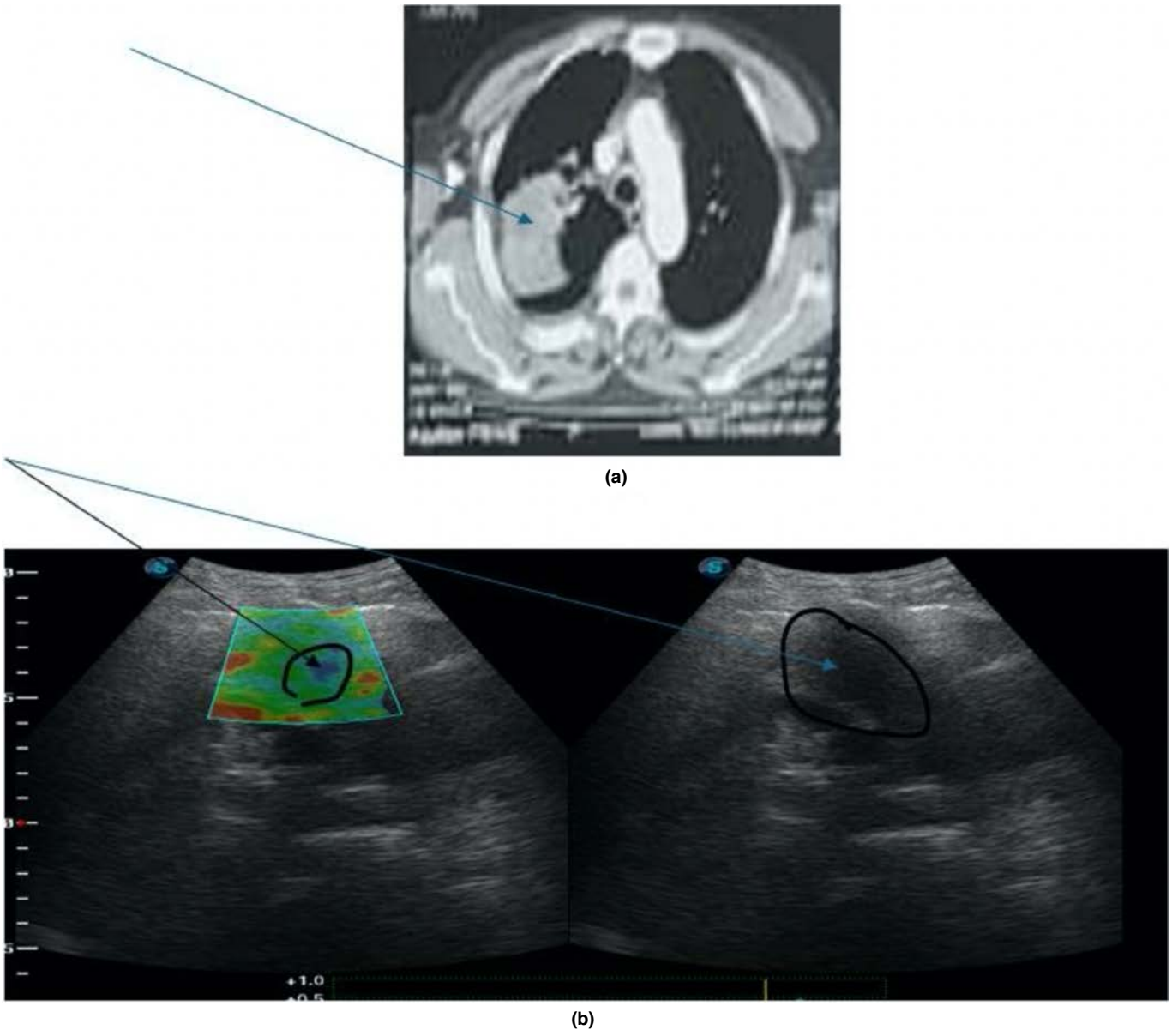

Figure 6: Computed tomography (CT) chest of a left soft tissue lesion with corresponding ultrasound elastography examination. Figure 6 describes a patient presenting with significant weight loss over two months and progressively worsening dyspnea. Transthoracic ultrasound-guided biopsy confirmed small cell lung carcinoma with a strain ratio (SR) of 2.34. (a) CT chest (mediastinal window) reveals a right peripheral soft tissue lesion. (b) B-mode ultrasound depicts an irregular, ill-defined hypoechoic lesion, while elastography highlights a hard lesion with a blue component

patients, followed by validation on two separate cohorts of 69 patients each. Similarly, in a study by Verhoeven et al.,[12] participants were randomly assigned, with 80% providing visual analog scores for SE, followed by performance evaluation on the remaining 20%.[21]

A wide range of SR values was observed, varying from 0.06 to 3.75 for patients with benign peripheral parenchymal lesions and from 1.75 to 5.0 for those with malignant lesions. This distribution suggests a statistically aberrant pattern, supporting the preference for median values over arithmetic means for improved accuracy in interpretation. The high SR values detected in benign peripheral lesions were attributed to either lung atelectasis or long-standing lung abscess, indicating underlying tissue alterations. Additionally, the presence of hard elastography patterns and high SR values in cavitary lesions and distal lung atelectasis contributed to the right-skewed statistical distribution observed in patients diagnosed with benign peripheral lesions.

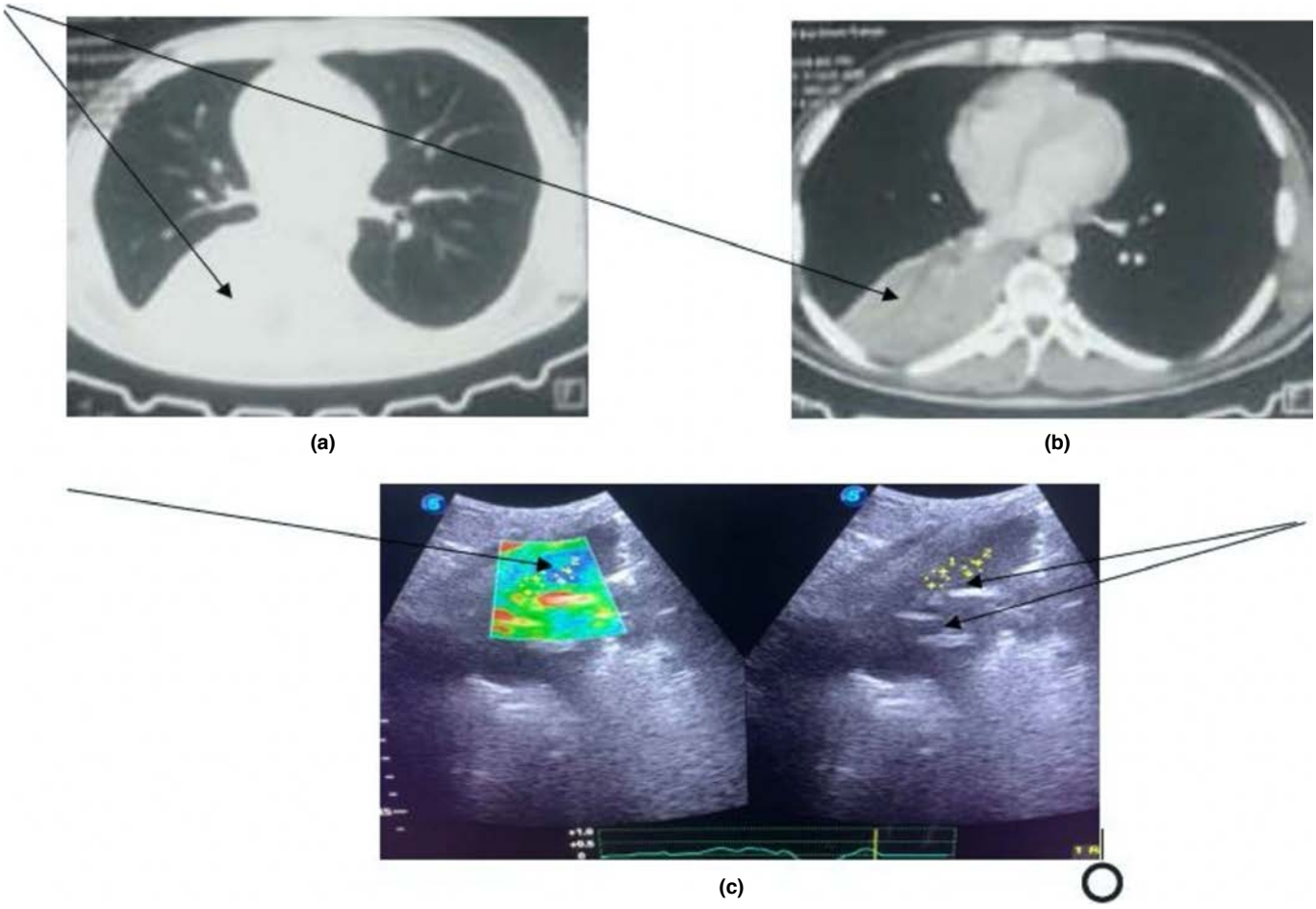

Figure 7: Computed tomography (CT) chest showing right lower lobe atelectasis with corresponding ultrasound elastography examination. (a) CT chest (lung window) and (b) mediastinal window reveal right lower lobe atelectasis. (c) B-mode ultrasound depicts a static air bronchogram, while elastography identifies the lesion as hard, despite the benign nature of the distal atelectasis. This case highlights a false positive in our study, as peripheral atelectasis can exhibit a hard component on elastography despite its benign nature, with a strain ratio (SR) of 1.92

A SR ≥1.75 suggests a higher likelihood of malignancy, with sensitivity of 98.67%, specificity of 82.54%, PPV of 87.1%, and NPV of 98.1%. The chosen cutoff value optimally balances sensitivity and specificity, as demonstrated by ROC curve analysis, yielding an area under the curve of 0.91 (95% CI: 0.85–0.97, p<0.0001).

The results align with the findings of Okasha et al.,[22] who identified an optimal SR cutoff value of 4.2 for assessing solid pancreatic lesions. Their approach demonstrated sensitivity of 97%, specificity of 63%, PPV of 89%, NPV of 88%, and accuracy of 89%. Notably, these outcomes closely resemble the performance metrics observed in our study.

Our study faced technical limitations, as it was conducted at a single center with a single operator, preventing an assessment of interobserver variability. Additionally, the absence of standardized elastography software resulted in SR variations, preventing the establishment of a definitive cutoff value for lesion differentiation.

Alternatively, Ozgokce et al.[23] investigated the use of shear-wave elastography (SWE) in distinguishing transudative from exudative pleural effusions, correlating their findings with Light's criteria. They reported excellent intraobserver reliability, with a reliability coefficient exceeding 85%, demonstrating strong consistency in SWE measurements when performed by the same observer across different sessions.

Challenges encountered during the study included frequent image freezing due to respiratory and vascular influences, particularly in overweight patients. Visualizing deeper pathologies proved difficult, and chronic inflammatory lesions exhibited increased stiffness, impacting specificity. Conversely, some malignant lesions demon-

strated lower stiffness, affecting sensitivity. Variability in establishing gold standard diagnoses across subjects was also noted, with criteria ranging from histopathology to clinical and radiological findings.

Conclusion

In conclusion, bedside ultrasound is highly valued for its accessibility and cost-effectiveness. Elastography techniques, such as SE and SR, are emerging approaches that play a crucial role in differentiating between hard and soft tissues, thereby enhancing tumor detection and diagnosis.

Ethics Committee Approval

The study was approved by the Alexandria University Ethics Committee (No: 0201692, Date: 16/06/2022).

Informed Consent

Informed consent was obtained from all participants.

Conflicts of Interest Statement

The authors have no conflicts of interest to declare.

Funding

The authors declared that this study received no financial support.

Use of AI for Writing Assistance

This work was produced without the assistance of artificial intelligence (AI)-assisted technologies, including large language models (LLMs), chatbots, or AI-based image creators.

Author Contributions

Concept – M.S.E.H., E.G.H., A.I.B., D.M.E., A.F.A.; Design – M.S.E.H., E.G.H., A.I.B., D.M.E., A.F.A.; Supervision – M.S.E.H., E.G.H., A.I.B., D.M.E., A.F.A.; Resource – D.M.E.; Materials – A.I.B.; Data collection &/or processing – M.S.E.H.; Analysis and/or interpretation – A.I.B.; Literature search – E.G.H.; Writing – M.S.E.H., A.I.B., D.M.E.; Critical review – M.S.E.H., A.I.B.

Acknowledgments

I would like to express my deepest gratitude to my supervisors for their invaluable guidance, support, and encouragement throughout this research. Their expertise and dedication have been instrumental in shaping the direction and quality of this work. I am also immensely grateful to Alexandria University for providing the resources and facilities necessary to conduct this study. This work would not have been possible without the support and contributions of everyone involved.

Peer-review

Externally peer-reviewed.

References

1. Liccardo B, Martone F, Trambaiolo P, Severino S, Cibinel GA, D'Andrea A. Incremental value of thoracic ultrasound in intensive care units: Indications, uses, and applications. World J Radiol 2016;8(5):460–71. [CrossRef]
2. Sigrist RMS, Liau J, Kaffas AE, Chammas MC, Willmann JK. Ultrasound elastography: Review of techniques and clinical applications. Theranostics 2017;7(5):1303–29. [CrossRef]
3. Demi L, Wolfram F, Klersy C, De Silvestri A, Ferretti VV, Muller M, et al. New international guidelines and consensus on the use of lung ultrasound. J Ultrasound Med 2023;42(2):309–44. [CrossRef]
4. Lee YH, Song HT, Suh JS. Use of strain ratio in evaluating superficial soft tissue tumors on ultrasonic elastography. J Med Ultrason (2001) 2014;41(3):319–23. [CrossRef]
5. Park HJ, Lee SY, Lee SM, Kim WT, Lee S, Ahn KS. Strain elastography features of epidermoid tumours in superficial soft tissue: Differences from other benign soft-tissue tumours and malignant tumours. Br J Radiol 2015;88(1050):20140797. [CrossRef]
6. Cui XW, Li KN, Yi AJ, Wang B, Wei Q, Wu GG, et al. Ultrasound elastography. Endosc Ultrasound 2022;11(4):252–74. [CrossRef]
7. Drakonaki EE, Allen GM, Wilson DJ. Ultrasound elastography for musculoskeletal applications. Br J Radiol 2012;85(1019):1435–45. [CrossRef]
8. Havre RF, Waage JER, Mulabecirovic A, Gilja OH, Nesje LB. Strain ratio as a quantification tool in strain imaging. Appl Sci 2018;8:1273. [CrossRef]
9. He HY, Chen JL, Ma H, Zhu J, Wu DD, Lv XD. Value of endobronchial ultrasound elastography in diagnosis of central lung lesions. Med Sci Monit 2017;23:3269–75. [CrossRef]
10. Kim SJ, Park HJ, Lee SY. Usefulness of strain elastography of the musculoskeletal system. Ultrasonography 2016;35(2):104–9. [CrossRef]
11. Boccatonda A, Susca V, Primomo GL, Cocco G, Cinalli S, Di Resta V, et al. Role of shear-wave and strain elastography to differentiate malignant vs benign subpleural lung lesions. Medicine (Baltimore) 2021;100(1):e24123. [CrossRef]
12. Verhoeven RLJ, de Korte CL, van der Heijden EHFM. Optimal endobronchial ultrasound strain elastography assessment strategy: An explorative study. Respiration 2019;97(4):337–47. [CrossRef]
13. Dietrich CF, Barr RG, Farrokh A, Dighe M, Hocke M, Jenssen C, et al. Strain elastography - How to do it? Ultrasound Int Open 2017;3(4):E137–49. [CrossRef]
14. Ozturk A, Grajo JR, Dhyani M, Anthony BW, Samir AE. Principles of ultrasound elastography. Abdom Radiol (NY) 2018;43(4):773–85. [CrossRef]
15. Lee H, Kim K, Lee Y. Development of stiffness measurement program using color mapping in shear wave elastography. Diagnostics (Basel) 2020;10(6):362. [CrossRef]
16. Lim CK, Chung CL, Lin YT, Chang CH, Lai YC, Wang HC, et al. Transthoracic ultrasound elastography in pulmonary lesions and diseases. Ultrasound Med Biol 2017;43(1):145–52. [CrossRef]
17. Sperandeo M, Trovato FM, Dimitri L, Catalano D, Simeone A, Martines GF, et al. Lung transthoracic ultrasound elastography imaging and guided biopsies of subpleural cancer: A preliminary report. Acta Radiol 2015;56(7):798–805. [CrossRef]
18. Wei H, Lu Y, Ji Q, Zhou H, Zhou X. The application of conventional us and transthoracic ultrasound elastography in evaluating peripheral pulmonary lesions. Exp Ther Med 2018;16(2):1203–8. [CrossRef]

19. Zhou B, Yang X, Zhang X, Curran WJ, Liu T. Ultrasound elastography for lung disease assessment. IEEE Trans Ultrason Ferroelectr Freq Control 2020;67(11):2249–57. [CrossRef]
20. Sperandeo M, Filabozzi P, Varriale A, Carnevale V, Piattelli ML, Sperandeo G, et al. Role of thoracic ultrasound in the assessment of pleural and pulmonary diseases. J Ultrasound 2008;11(2):39–46. [CrossRef]
21. Hahn S, Lee YH, Lee SH, Suh JS. Value of the strain ratio on ultrasonic elastography for differentiation of benign and malignant soft tissue tumors. J Ultrasound Med 2017;36(1):121–7. [CrossRef]
22. Okasha HH, Mahdy RE, Elkholy S, Hassan MS, El-Mazny AN, Hadad KEE, et al. Endoscopic ultrasound (EUS) elastography and strain ratio, could it help in differentiating malignant from benign pancreatic lesions? Medicine (Baltimore) 2018;97(36):e11689. [CrossRef]
23. Ozgokce M, Durmaz F, Yavuz A, Üney İ, Yildiz H, Arslan H, et al. Shear-wave elastography in the characterization of pleural effusions. Ultrasound Q 2019;35(2):164–8. [CrossRef]